

HIERARCHICAL EVALUATION MODEL FOR 3D FACE RECOGNITION

Sídnei A. Drovetto Jr., Luciano Silva and Olga R. P. Bellon
IMAGO Research Group, Universidade Federal do Paraná, Curitiba - PR, Brazil

Keywords: Face recognition, Simulated Annealing, 3D image registration, Surface Interpenetration Measure.

Abstract: In this paper we propose to perform 3D face matching based on alignments obtained using Simulated Annealing (SA) algorithm guided by the Mean Squared Error (MSE) with M-estimator Sample Consensus (MSAC) and the Surface Interpenetration Measure (SIM). The matching score is obtained by calculation of the SIM after the registration process. Since the SIM is a sensitive measure, it needs a good alignment to give relevance to its value. Our registration approach tends to reach a near global solution and, therefore, produces the necessary precise alignments. By analyzing the matching score, the system can identify if the input images come from the same subject or not. In a verification scenario, we use a hierarchical evaluation model which maximizes the results and reduces the computing time. Extensive experiments were performed on the well-known Face Recognition Grand Challenge (FRGC) v2.0 3D face database using five different facial regions: three regions of the nose; the region of the eyes; and the face itself. Compared to state-of-the-art works, our approach has achieved a high rank-one recognition rate and a high verification rate.

1 INTRODUCTION

Recently, some approaches for 3D face recognition have used image registration to measure the similarity between faces, often based on MSE or Root Mean Squared Error (RMSE) (Chang et al., 2006; Chang et al., 2005; Lu and Jain, 2005; Lu et al., 2006). In all these approaches, Iterative Closest Point (ICP) is traditionally applied as the registration method. However, ICP demands good initial pre-alignment to be successfully applied, which is not adequate for an automatic approach. Also, ICP is guided by the MSE but it was proved (Silva et al., 2005a) that this measure could allow imprecise local convergence for range image registration, even when improved ICP-based approaches are used (Rusinkiewicz and Levoy, 2001; Gelfand et al., 2003). In addition, in (Silva et al., 2005a) the authors suggest that MSE is a good measure for starting the image registration process, but SIM could be more suitable to be used at “the end of the game” to assess the quality of the registration.

To surpass these limitations, we developed an approach for 3D face registration that uses the SIM (Silva et al., 2005a) to measure the similarity between facial regions. Also, since SIM is a sensitive measure, a good final alignment is required for it to produce a reliable value. Then, this precise align-

ment is achieved using a SA based approach for image registration. In the last stage of the registration process, the goal of SA is to maximize SIM and, therefore, the similarity between the faces can be reliably calculated. Very extensive results and comparisons between ICP and SIM-based registration approaches can be found in (Silva et al., 2005b).

The two main functionalities of biometric systems are handled in different ways in our approach. First, for the verification scenario, we employ a hierarchical evaluation model that analyzes, separately, only the segmentation results that are relevant to make the correct decision. Then, for the recognition scenario, the matching score is calculated for each segmentation result and after that, all of them are combined into one score that is used for identification.

Extensive experiments were performed on the well-known FRGC v2.0 3D face database. The experimental results showed that our approach produces good results for both recognition and verification scenarios when compared to state-of-the-art works (Chang et al., 2006; Chang et al., 2005; Lu and Jain, 2005; Lu et al., 2006).

This paper is organized as follows. First, in section 2, we review some related works. Next, we introduce our 3D face matching approach in section 3. For a verification scenario, we have adopted a hi-

erarchical evaluation model that is described in section 4. The experimental results summarizing the obtained rates for recognition and verification problems are presented in section 5, followed by the final remarks in section 6.

2 RELATED WORKS

In (Chang et al., 2006; Chang et al., 2005) the authors propose the use of three overlapping regions around the nose — circular nose region, elliptical nose region and nose region — to overcome the facial expression problem, since these regions are approximately rigid across expression variation. The matching score for each region are combined to improve the accuracy. The steps involved in this approach are: (1) face extraction: using skin detection applied to the 2D image; (2) curvature based segmentation and landmark detection; (3) pose correction: the extracted face is aligned, using ICP, to a generic 3D face model; (4) extraction of nose regions based on the landmarks; (5) registration of surfaces: the registration is accomplished by ICP and the matching score is the resulting RMSE.

Combining the three nose regions, this approach achieved a rank-one recognition rate of 97.1% and a Equal Error Rate (EER) of approximately 0.12% using only neutral expression images (Chang et al., 2006). The neutral expression database used in the experiments consists of 2,798 images of 546 subjects. The images were divided into one gallery, with 449 images, and nine probe sets totalizing 2,349 images.

In (Lu and Jain, 2005; Lu et al., 2006) the 2D and 3D images are used to perform face recognition. ICP is used to match the 3D data and Linear Discriminant Analysis (LDA) employed to match the 2D images. The combination of the values is done using the weighted sum rule (Kittler et al., 1998). This approach is composed by three steps: (1) coarse alignment based on feature points (obtained manually); (2) fine alignment: using a modified version of ICP which alternates point-to-point distance (Besl and McKay, 1992) and point-to-plane distance (Chen and Medioni, 1992); (3) LDA match on a dynamically generated gallery; (4) integration. The matching score for the 3D data is the RMSE of the point-to-plane distance provided by ICP.

By integrating ICP and LDA matching scores, this approach obtained a rank-one recognition rate of 99% using only neutral expression frontal face views. The gallery is composed by 200 3D face models and the probe has 99 neutral expression frontal images.

As we can see, both approaches are based on RMSE values provided by ICP and achieve a high

rank-one recognition rate. Also, both approaches have performed experiments using images containing facial expressions, but their best results, presented above, were obtained using only neutral expression images.

3 3D FACE MATCHING

We propose to perform 3D face matching by combining a precise registration technique and the SIM (Bellon et al., 2006) to evaluate different facial regions. The registration is obtained by a SA based approach, which have two important advantages: (1) it tends to find a near global solution; (2) it can be easily integrated with different kinds of estimators. We use two robust measures in our SA approach. First the MSAC is combined with the MSE for a coarse alignment and latter SIM is applied to achieve a fine registration. The matching score is given by the SIM value of the final alignment for the two images. The SIM is used as matching score because it produces a better range for discrimination between faces, when compared to other metrics.

3.1 The Surface Interpenetration Measure

The SIM was developed by analyzing visual results of two aligned surfaces, each rendered in a different color, crossing over each other repeatedly in the overlapping area (Silva et al., 2005b). The interpenetration effect results from the nature of real range data, which presents slightly rough surfaces with small local distortions caused by limitations of the acquiring system. Because of this, even flat surfaces present a “roughness” in range images. With this, we can assume that independently of the shape of the surfaces the interpenetration will always occur. It was also observed that two images acquired from the same object surface using the same scanner position and parameters provide two different range images.

By quantifying interpenetration, one can evaluate more precisely the registration results and provide a highly robust control (Silva et al., 2005a). To do this it was developed the following measure based on the surface normal vector, computed by a local least squares planar fit, at each point. After the alignment of two images, A and B , it is identified the set of interpenetrating points in A with respect to B . For each point $p \in A$ it is defined a neighborhood N_p as a small $n \times n$ window centered on p . With q denoting a point in the neighborhood N_p , c the corresponding point of p in image B and \vec{n}_c the local surface normal at c , the

set of interpenetrating points is defined as:

$$C_{(A,B)} = \{p \in A \mid [(\vec{q}_i - \vec{c}) \cdot \vec{n}_c][(\vec{q}_j - \vec{c}) \cdot \vec{n}_c] < 0\} \quad (1)$$

where $q_i, q_j \in N_p$ and $i \neq j$. This set comprises those points in A whose neighborhoods include at least one pair of points separated by the local tangent plane, computed at their correspondents in B , as can be seen in the diagram of Figure 1.

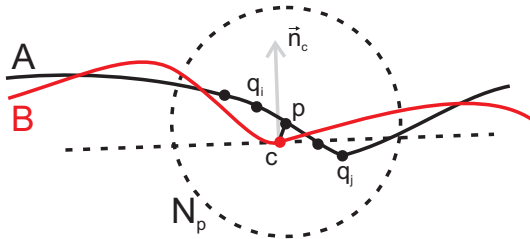


Figure 1: Interpenetrating point p in A with respect to B .

With this, the SIM is defined as the fraction of interpenetrating points in A :

$$SIM_{(A,B)} = \frac{|C_{(A,B)}|}{|A|} \quad (2)$$

In this paper some constraints were applied to the SIM as suggested in (Silva et al., 2005b) to avoid incorrect corresponding points, and to obtain more precise alignments. It was included the constraint $m = 5$ as the maximum angle allowed between the normal vectors at c and p , \vec{n}_c and \vec{n}_p , respectively. Then, we have $p \in C$ only if $\cos^{-1}(\vec{n}_c \cdot \vec{n}_p) \leq m$. Also, it was used a constraint to eliminate the corresponding points on the surfaces boundaries. In this case, $p \in C$ if $c \notin D$, where D is the set of boundary points in B , and the thickness of the boundary defined as $s = 1$;

Registrations of two range images presenting good interpenetration have high SIM values. The experimental results show that erroneous alignments produce low SIM values and that small differences in MSE can yield significant differences in SIM. Furthermore, alignments with high SIM present a very low interpoint distance between the two surfaces. That is, SIM is a far more sensitive indicator of alignment quality when comparing “reasonable” alignments (Silva et al., 2005a; Bellon et al., 2005).

3.2 SA-Based Registration

SA (Kirkpatrick et al., 1983) is a stochastic algorithm for local search in which, from an initial candidate solution, it generates iterative movements to a neighbor solution that represents a better solution to the problem as compared to the current one. The main difference between SA and other local search algorithm,

e.g. Hill Climbing, is that SA can accept a worse solution than the current candidate in the iterative process. Then, SA does not remain “tied” to local minima and because of this it has better chances to reach its goal, which is a solution close enough to the global one.

In order to apply SA on registration of two range images, six parameters (three parameters each for rotation and translation relative to a 3D coordinate system) are needed to define the candidate solutions as a “transformation vector” that, when applied to one image, can align it with the other.

Our SA-based approach was developed using the GSL Library¹ adopting a coarse-to-fine strategy and has three main stages: (1) pre-alignment; (2) coarse alignment; (3) fine alignment.

3.2.1 Pre-Alignment

Before starting the registration process, an initial solution is required. Instead of using a random solution to start our method, we choose the best one among three pre-alignments, which are: (a) center of mass; (b) nose tip; (c) bounding box center — to avoid incorrect nose tip localization due to noise points, this landmark is defined as the center of the closest 3×3 window to the sensor. In order to evaluate the convergence behavior of each pre-alignment, few iterations of the SA, only 75 based on our experiments, are performed, using the cost function of the coarse alignment stage to guide the evaluation process. This evaluation is done to find the pre-alignment that has the fastest convergence. The selected pre-alignment represents a good starting point for the algorithm, which can lead to a faster and better convergence.

3.2.2 Coarse Alignment

In this stage the SA-based searching procedure uses MSAC (Torr and Zisserman, 2000) combined with MSE of corresponding points between two images as the cost function to obtain a coarse alignment. The nearest-neighbor criterion is used to establish correspondence between points of each image — the search is performed using a KD-tree structure.

Based on a threshold applied on the associated error of corresponding points — in our case MSE is the error measure — the MSAC classifies corresponding points either as inliers or outliers. The error associated to outliers is a fixed penalty and to the inliers is the error measure itself, squared. That means, they are scored on how well they fit the data (Torr and Zisser-

¹GNU Scientific Library - <http://www.gnu.org/software/gsl>

man, 2000). The MSAC definition is given by Eq. 3.

$$\rho_2(e^2) = \begin{cases} e^2 & e^2 < T^2 \\ T^2 & e^2 \geq T^2 \end{cases} \quad (3)$$

where e is the error of corresponding points and T is the threshold.

By reducing the error associated to the outliers, we minimize their influence on the registration process and, therefore, a better alignment can be obtained.

In order to speed up this stage, only 3% of the valid points are used. Our experiments have shown that this sampling rate does not risk the coarse alignment.

The initial solution of this stage is the best solution found in the iterations performed on the pre-alignments of the previous stage. The “temperature” of SA is reduced very slowly and only one iteration is performed for each allowed “temperature” as suggested by (Lundy and Mees, 1986). This stage ends when no better solution is found within 350 consecutive iterations of SA, based on our experiments this condition is a compromise between a good coarse alignment and a small computing time. The movements to neighbor solutions across each iteration is done by the introduction of small random values within $[-1, 1]$ to each element of the transformation vector. The initial “temperature” was defined as $t_0 = 0.002$. At this “temperature” and using MSAC as the cost function, approximately 60% of worse solutions are accepted. According to (Rayward-Smith et al., 1996) it is a criterion that should be met for the initial “temperature”. The threshold value for MSAC was empirically defined as $T = 0.7$, which represents an inlier boundary distance for the corresponding points between images.

3.2.3 Fine Alignment

In this stage the cost function for the SA-based searching procedure is the SIM calculated over 9% of the image valid points. Our experiments, see Fig. 2, have shown that SIM at this sampling rate, comparing to SIM using all points, presents an average variation of approximately 2%. Therefore, the increase of speed compensates the small inaccuracy. We have used 200 face alignments to produce Fig. 2. For each alignment it was calculated the relative error of SIM using sampling rates varying from 1% to 99%, when compared to SIM using all points.

The initial solution of this stage is the best solution found on the previous stage. Again, the cooling schedule proposed by (Lundy and Mees, 1986) was used. In an attempt to move to a better neighbor solution, random values within $[-0.0667, 0.0667]$ are introduced to each element of the transformation

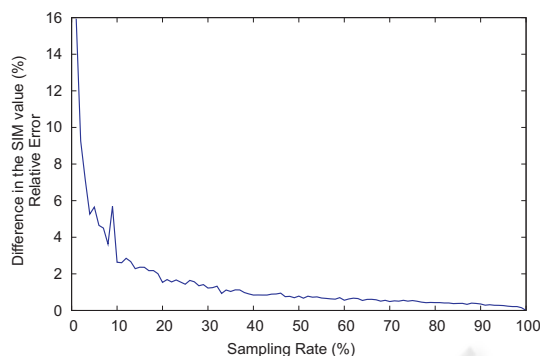


Figure 2: Relative error of SIM using a sampling rate when compared to SIM using all points.

vector. These values are smaller than the ones in the previous stage because a good alignment has already been achieved and we only want to make minor movements in order to improve it. The initial “temperature” was defined as $t_0 = 0.15$, again we have employed the method suggested by (Rayward-Smith et al., 1996). This stage ends when the solution is not improved in 40 consecutive iterations of SA, as in the previous stage. This condition is a compromise between a precise alignment and a small computing time.

4 HIERARCHICAL EVALUATION MODEL AND FACIAL REGIONS

We have used five facial regions (Fig. 3) in our hierarchical evaluation model: nose region (NR), elliptical nose region (NE), circular nose region (NC), eyes region (ER) and face region (FA). The three nose regions were suggested in (Chang et al., 2006; Chang et al., 2005) and are described to be relatively insensitive to facial expressions. These three regions are also important when using only neutral expression faces because, even if a subject is asked to make a neutral expression at two different times, the 3D face shape will still be different by some amount (Chang et al., 2006).

The hierarchical evaluation model, see Fig. 4, is used in a verification scenario. This model consists in analyzing one region only when the matching score of a previously analyzed one was not sufficient to determine whether the images belong to the same subject or not. The classification of the images is based on two thresholds: (1) a recognition threshold; (2) a rejection threshold. If the matching score is higher than the recognition threshold, the images are assumed to belong to the same subject (client), however if it is

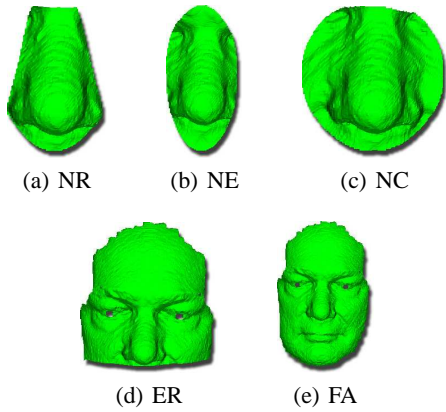


Figure 3: Facial regions used in our evaluation model.

lower than the rejection threshold the images are labeled as belonging to different subjects (impostor). In case the matching score lies between the thresholds, no affirmation can be made and the next region of the hierarchy is used in another attempt to classify the images. After obtaining all the matching scores, the thresholds are automatically defined in a way that no client score is below the rejection threshold and no impostor score is above the recognition threshold. This model has two purposes: (1) achieve high verification rates; (2) keep a small execution time.

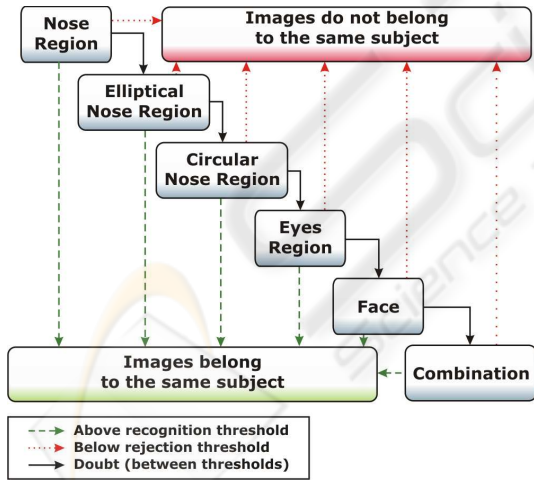


Figure 4: Proposed Hierarchical Evaluation Model.

Since the regions vary greatly in size, the order in which they are evaluated plays a very important role in keeping execution time as small as possible. The execution goes from the smallest region, NR, to the largest one, FA. By doing this, the average execution time of the algorithm tends to be near the time necessary to match the smaller regions. In the last level of

the hierarchy, the combination, which is a weighted mean of the matching scores of previous levels, is compared against a single threshold and the pair of images is classified as client or impostor.

This model increases the verification rate because sometimes one single region can lead to the correct result while the combination of all the regions cannot. This particular situation can happen if one of the images has hair occlusion, noisy regions or expression.

5 EXPERIMENTAL RESULTS

The experiments were performed using 978 images from the well-known FRGC v2.0 database (Phillips et al., 2005). Each image of the database, acquired by a Minolta Vivid 900/910 series sensor, has 640×480 pixels and was divided according to the presence of noise and expression. We have applied our approach in the group that satisfies two criteria: (1) neutral or minor expression; (2) little or no noise perturbation from the acquisition process. This group contains 978 images and it was used to establish a baseline for our approach in a controlled environment. We matched each image against all others, totalizing 477,753 combinations (475,091 from different subjects and 2,262 from the same subject). Using the method proposed in (Segundo et al., 2007), each image was automatically segmented into the five used regions.

Fig. 5 presents five face matching where each image was rendered using different colors to show the interpenetrating areas. We can observe some particular cases, as in Fig. 5 (a) where the forehead is partially occluded due to hair, or in Fig. 5 (p) where the subject was using a bandanna that was not removed by the segmentation algorithm. However, in both cases, the SIM value for the alignment was enough for a correct classification of the images.

By using the hierarchical evaluation model we have achieved a verification rate of 99.77% at a False Acceptance Rate (FAR) of 0% which means that in a verification system, no impostor would be accepted as a client. Table 1 presents the number of combinations, rejection and recognition thresholds regarding the execution of our evaluation model for the used dataset. After the last threshold is applied, only 6 combinations out of 477,753 are misclassified and, since we are using a FAR of 0%, the 6 combinations are all false rejection cases. In Fig. 5 (u) – (y) it is presented one case where the matching score was not high enough for a correct classification. Fig. 6 shows the variation of FAR and False Rejection Rate (FRR) according to threshold variations. By analyz-

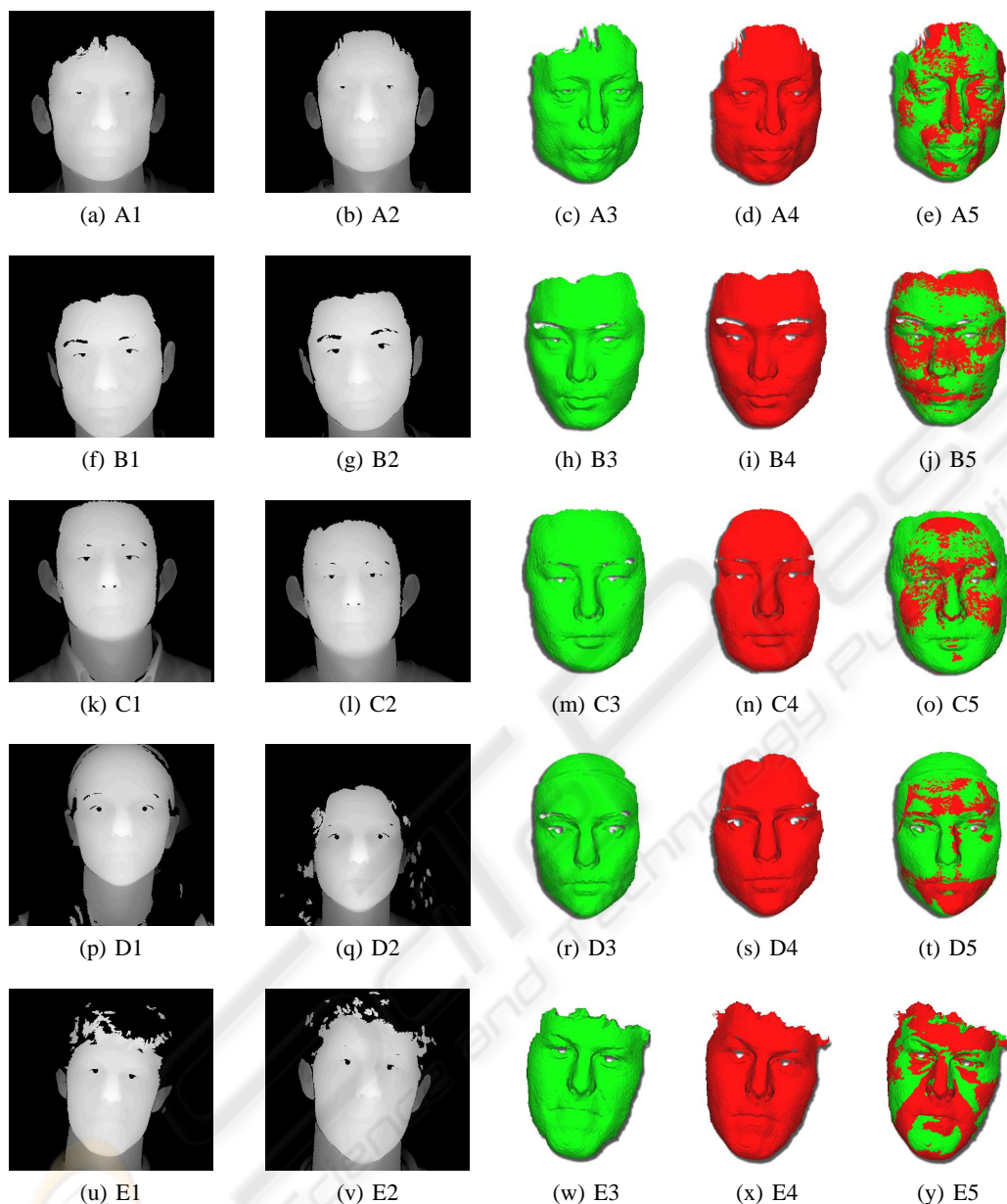


Figure 5: Examples of facial alignments obtained by our registration method: X_1 and X_2 are raw images from the database; X_3 is the rendered face segmentation of X_1 ; X_4 is the rendered face segmentation of X_2 ; X_5 is the alignment of X_3 and X_4 ; (e) final SIM value 41.38%; (j) final SIM value 45.34%; (o) final SIM value 47.11%; (t) final SIM value 22.34%; (y) final SIM value 8.54%.

ing this figure we can see that the overlapping area of the curves is very small, indicating that the scores of clients and impostors are rarely mixed up.

Fig. 7 shows the Receiver Operating Characteristic (ROC) curve, which demonstrates the trade-off between the FAR and the FRR. We can see that with such rates, in a verification scenario the system would have either secure (small FAR) and

convenient (small FRR) behavior. In Figs. 6 (b) and 7 we can see the point at which FAR equals FRR, this point is called EER and, it is approximately 0.033% for our approach.

For the assessment of the algorithm in a recognition scenario, the images were randomly divided into three sets: one gallery and two probes. The gallery set contains 256 images, one for each subject in the

Table 1: Hierarchical evaluation using the five segmentations and their combination.

Region	Nr. Comb.	Rejec. T.	Recog. T.
NR	477,753	1.32%	29.60%
NE	427,505	0.82%	24.43%
NC	412,398	2.73%	23.31%
ER	253,642	5.94%	14.10%
FA	11,469	4.48%	10.09%
Comb.	5,102	11.71%	

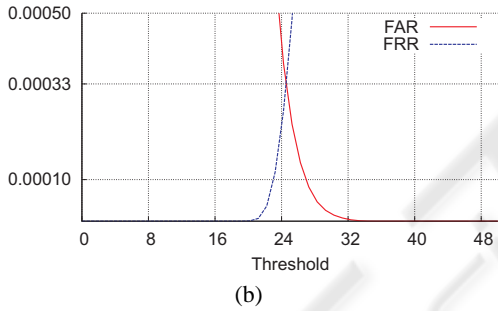
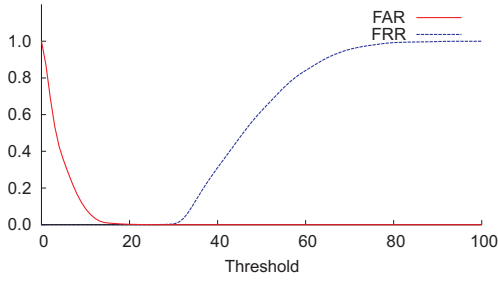


Figure 6: FAR and FRR curves: (a) FAR and FRR curves for all possible thresholds; (b) approximation of the crossing region.

database, and each probe set contains 361 images. By combining the results for each region, in the same way it was done for the verification scenario, we have reached a rank-one recognition rate of 100%. The rank-one recognition rate and the Cumulative Match Characteristic (CMC) curves for each facial region and their combination are given in Table 2 and Fig. 8, respectively.

6 CONCLUSIONS AND FUTURE WORK

We have presented a robust approach for 3D face matching based on SA, SIM and a hierarchical evaluation model. We propose the use of a precise reg-

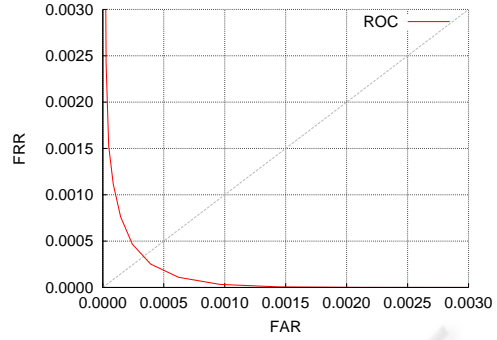


Figure 7: Receiver Operating Characteristic curve.

Table 2: Rank-one recognition rate for each individual region and their combination.

Region	Rank-One Recognition Rate		
	Probe 1	Probe 2	Average
NR	95.29%	97.78%	96.53%
NE	98.33%	98.61%	98.47%
NC	98.33%	98.89%	98.61%
ER	99.72%	99.44%	99.58%
FA	98.89%	99.16%	99.03%
Comb.	100.00%	100.00%	100.00%

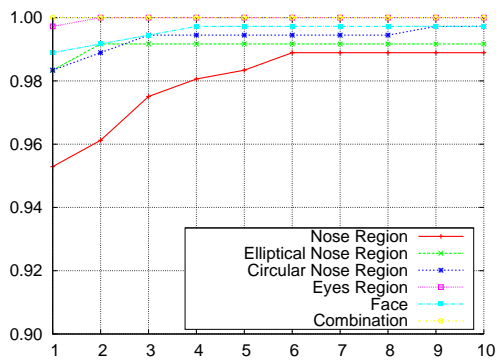
istration method and the SIM as a matching score to verify similarity between face regions. The registration follows a coarse-to-fine strategy, first employing the MSE constrained by the MSAC as the cost function of SA and then, the SIM as the cost function in order to obtain a refined alignment. The adopted evaluation model aims to minimize the execution time and to maximize the verification rate.

The experimental results have shown the effectiveness of our approach for both recognition and verification scenarios. For the recognition problem, our approach achieved a rank-one recognition rate of 100%. The rates for the verification scenario are also very high, 99.77% for the verification rate at a FAR of 0% and approximately 0.033% for the EER.

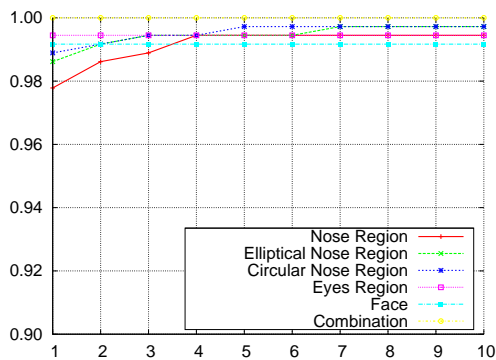
As a future work we plan to study the effects of facial expressions on the proposed approach and, if necessary, employ techniques that minimize them.

ACKNOWLEDGEMENTS

The authors would like to thank Dr. Jonathon Phillips and Dr. Patrick Flynn for allowing us to use the images; and Conselho Nacional de Desenvolvimento Científico e Tecnológico (CNPq) for financial support.



(a) CMC curves for probe 1



(b) CMC curves for probe 2

Figure 8: Cumulative Match Characteristic curves for each region and their combination: (a) for probe set 1; (b) for probe set 2.

REFERENCES

- Bellon, O. R. P., Silva, L., Queirolo, C., Drovetto, S., and Pamplona, M. (2006). 3d face image registration for face matching guided by the surface interpenetration measure. In *ICIP*, pages 2661–2664. IEEE.
- Bellon, O. R. P., Silva, L., and Queirolo, C. C. (2005). 3D face matching using the surface interpenetration measure. In *Lecture Notes in Computer Science*, volume 3617, pages 1051–1058. Springer-Verlag.
- Besl, P. J. and McKay, N. D. (1992). A method for registration of 3-D shapes. *IEEE Trans. Pattern Analysis and Machine Intelligence*, 14(2):239–256.
- Chang, K. I., Bowyer, K. W., and Flynn, P. J. (2005). Adaptive rigid multi-region selection for handling expression variation in 3D face recognition. In *Proc. of IEEE Conf. CVPR*, volume 3, pages 157–164.
- Chang, K. I., Bowyer, K. W., and Flynn, P. J. (2006). Multiple nose region matching for 3d face recognition under varying facial expression. *IEEE Trans. Pattern Analysis and Machine Intelligence*, 28(10):1695–1700.
- Chen, Y. and Medioni, G. (1992). Object modelling by registration of multiple range images. *Image Vision Computing*, 10(3):145–155.
- Gelfand, N., Ikemoto, L., Rusinkiewicz, S., and Levoy, M. (2003). Geometrically stable sampling for the ICP algorithm. In *Proc. of 4th Intl. Conf. on 3D Digital Imaging and Modeling*, pages 260–267.
- Kirkpatrick, S., Gelatt, C. D., and Vecchi, M. P. (1983). Optimization by simulated annealing. *Science*, 220(4598):671–680.
- Kittler, J., Hatef, M., Duin, R. P. W., and Matas, J. (1998). On combining classifiers. *IEEE Trans. Pattern Analysis and Machine Intelligence*, 20(3):226–239.
- Lu, X. and Jain, A. K. (2005). Integrating range and texture information for 3d face recognition. In *Proc. of 7th IEEE Workshop on Applications of Computer Vision*, pages 156–163.
- Lu, X., Jain, A. K., and Colbry, D. (2006). Matching 2.5D face scans to 3D models. *IEEE Trans. Pattern Analysis and Machine Intelligence*, 28(1):31–43.
- Lundy, M. and Mees, A. (1986). Convergence of an annealing algorithm. *Mathematical Programming: Series A and B*, 34(1):111–124.
- Phillips, P. J., Flynn, P. J., Scruggs, W. T., Bowyer, K. W., Chang, J., Hoffman, K., Marques, J., Min, J., and Worek, W. J. (2005). Overview of the face recognition grand challenge. In *Proc. of IEEE CVPR*, pages 947–954.
- Rayward-Smith, V. J., Osman, I. H., Reeves, C. R., and Smith, G. D. (1996). *Modern Heuristic Search Methods*. John Wiley & Sons Ltd.
- Rusinkiewicz, S. and Levoy, M. (2001). Efficient variants of the ICP algorithm. In *Proc. of 3rd Intl. Conf. on 3D Digital Imaging and Modeling*, pages 145–152.
- Segundo, M. P., Queirolo, C. C., Bellon, O. R. P., and Silva, L. (2007). Automatic 3d facial segmentation and landmark detection. *XIV Intl. Conf. on Image Analysis and Processing*, pages 431–436.
- Silva, L., Bellon, O. R. P., and Boyer, K. L. (2005a). Precision range image registration using a robust surface interpenetration measure and enhanced genetic algorithms. *IEEE Trans. Pattern Analysis and Machine Intelligence*, 27:762–776.
- Silva, L., Bellon, O. R. P., and Boyer, K. L. (2005b). *Robust Range Image Registration Using Genetic Algorithms and the Surface Interpenetration Measure*, volume 60 of *Machine Perception and Artificial Intelligence*. World Scientific Publishing.
- Torr, P. H. S. and Zisserman, A. (2000). MLESAC: A new robust estimator with application to estimating image geometry. *CVIU*, 78:138–156.